33rd Annual International Conference of the IEEE EMBS
Boston, Massachusetts USA, August 30 - September 3, 2011

Automatic estimation of pelvic organ anatomical references

Mehdi Rahim, Marc-Emmanuel Bellemare, Nicolas Pirró, Rémy Bulot

Abstract— **Pelvic floor diseases cover pathologies of which physiopathology is not well understood. 2D sagittal MRI sequences used in the clinical assessment allow to visualize the dynamic behavior of the main organs involved (bladder, uterus-vagina and rectum). Clinicians use anatomical landmarks and measurements related to the pelvic organs in their pathology assessment. Usually, those tasks are performed manually which results in being both tedious and subject to operator dependency. A methodology is proposed to attempt a quantitative and objective characterization of the organ behaviors under abdominal strain condition. This approach automatically assesses the organ movements, through the estimation of characteristic angles (anorectal angle, uterovaginal angle, bladder inclination), and the tracking of anatomically significant points (anorectal angle vertex, uterovaginal angle vertex, bladder neck). From a multi-subject analysis, pathological organs have been distinguished from healthy ones, which shows the relevance of the computed features. In addition, a stability analysis has shown the soundness of the approach.**

I. INTRODUCTION

Pelvic floor disorders cover pathologies that associate a loss of normal anatomical link of pelvic organs, leading to altered anorectal or urogenital functions and degraded life quality. Those pathologies result from different factors such as aging, pregnancy, obesity, injuries, or a combination of them. They concern mainly a growing population of old people, 60% of 60 years old women are concerned by those troubles. They are considered as a public health issue in several countries. Although significant research has been performed, the pelviperineal physiology and the anatomic basis of pelvic floor diseases remain unclear, as mentioned in [8] and [4].

Dynamic magnetic resonance (MRI) sequences ($2D+t$) allow the visualization of the organs under strain condition. This acquisition technique is routinely used to perform the diagnosis. The main soft tissue organs involved are the bladder, the uterus, the vagina and the rectum. In addition, some muscles and rigid structures are observed, such as the perineum, the coccyx and the pubic symphysis. Radiologists analyze the displacement and the deformation of the pelvic organs to assess the pathology grade [2], [7]. They assume that the most relevant observation of the pelvic organ dynamics is done within the median sagittal plane. Even though partial, this latter is the only dynamic acquisition available in clinical routine. The movements in the coronal and transverse planes are limited and can be considered as negligible.

The pelvic floor disorders are characterized by large organ deformations and abnormal organ descents during the strain. In a previous work [5], the organ deformations were estimated by using quantitative shape descriptors, giving a global information about the organ behaviors.

Furthermore, clinicians use anatomically meaningful landmarks and measurements to characterize the posture of an organ, and to analyse its evolution along a sequence. However, this task requires a manual intervention of the clinician, which is time-consuming, specially on the whole MR images of several sequences. It is also prone to the subjectivity of the operator. In [1], the authors show the limitations of the manual measurements of the anorectal angle, resulting in high rates of the inter-operator variability. Therefore, the aim of this study is to perform an objective and reproducible approximation of the anatomical references, starting from the organ contours extracted from a dynamic MRI sequence, by analyzing the geometrical properties of the shape of the organs. In addition to their relevance for the discrimination between the behavior of healthy and diseased organs, the stability of these estimators is assessed, by performing an inter-sequence analysis.

The segmentation process is out of the scope of this study, resulting DICOM images were segmented by clinicians providing a set of closed contours of each of the three organs of interest (bladder, uterus-vagina, rectum), as depicted in figure 1.

We detail in section II the proposed approach for the landmark computation of each organ. Some results are presented in section III, where the pathology detection capability of the computed features is analysed, in addition to the feature robustness towards organ segmentation variability. Section IV concludes the paper.

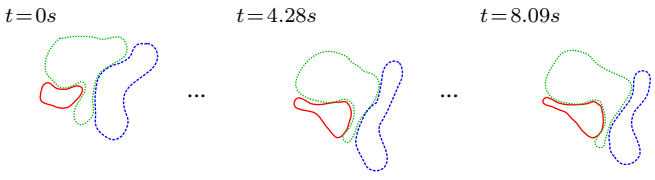

Fig. 1. A Segmented MRI Sequence

II. PELVIC LANDMARK APPROXIMATION

A simple way to assess an organ movement boils down to compute its center of mass on each sequence frame in order to build a trajectory. Nevertheless, the center of gravity is a global measurement, it does not take into account the local behavior specific to the anatomical references. Moreover, the

M. Rahim is with LSIS Laboratory (UMR CNRS 6168), Aix-Marseille University, Marseille, France mehdi.rahim@lsis.org
M.-E. Bellemare is with LSIS Laboratory (UMR CNRS 6168), Aix-Marseille University, Marseille, France
N. Pirró is with the Digestive Surgery Department, La Timone Hospital, Marseille, France
R. Bulot is with LSIS Laboratory (UMR CNRS 6168), Aix-Marseille University, Marseille, France

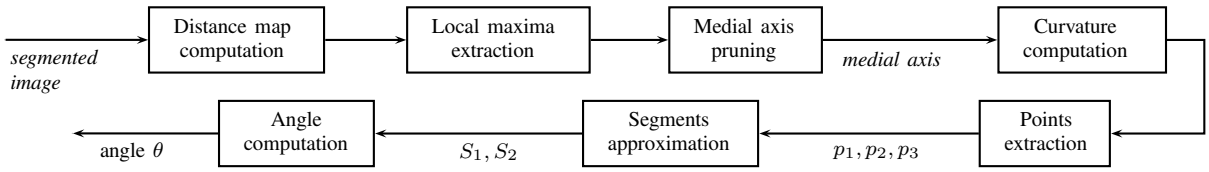

Fig. 2. Anatomical Reference Approximation Flowchart.

trajectories are sensitive to the patient movements during the sequence acquisition process. Hence, another interest in the computation of anatomical references is to overcome those issues.

There are two kinds of anatomical landmarks: fixed landmarks and mobile ones. The fixed landmarks are defined with respect to the pelvic rigid structures whose movements and deformations are almost nil. Typically, the bone structures are used as references. For instance, the sub-pubo-coccygean line (SPCL) is a virtual line, it encloses the lower edge of the pubic symphysis to the end of the sacrum, it is a landmark assumed to be static.

The mobile landmarks are related to soft-tissue organs which undergo deformations during an abdominal strain. The following list summarizes the angles and points related to the three pelvic organs:

- *Rectum* : Anorectal angle and vertex.
- *Uterus-vagina* : Uterovaginal angle and vertex.
- *Bladder* : Bladder inclination and bladder neck.

In the following subsections, we describe for each organ the computation methods of the points and the angles. A typical result is depicted with figure 3-b.

A. Rectum

The anorectal angle is the junction of the rectum with the anus, we compute this angle by exploiting the curvature properties of the rectum medial axis, three points which form the anorectal angle are then determined.

Figure 2 summarizes the angle computation steps which are detailed below.

1) Distance map computation: The distance map is computed on a binary image yielding a real valued matrix DM. For each pixel p of a binary shape P :

$$DM(p) = \min_k \{d(p, q_k) : P(q_k) = 0 \wedge 1 \leq k \leq S\}$$

where k lists the image pixels S, and d the Euclidean distance. In our experiments, the distance map was computed with a 5×5 Chamfer mask as advocated in [6].

2) Medial Axis extraction: A rough medial axis is extracted thanks to the distance map (DM) local maxima estimation. A pruning step is applied on this medial axis. Then, a central line (point coordinates) is extracted by removing the bifurcations.

3) Medial Axis curvature computation: In order to extract the characteristic angle, the curvature of the medial axis is estimated at each point. A pre-processing step is required to obtain an ordered medial axis curve P consisting of points $p(t) = (x(t), y(t))$. Then, the curvature $k(t)$ is computed :

$$k(t) = \frac{x'(t)y''(t) - y'(t)x''(t)}{(x'(t)^2 + y'(t)^2)^{3/2}}$$

In order to limit the discretization noise influence on the curvature estimation, we performed a light Gaussian based smoothing of the central line before the computation.

4) Angle approximation: The three angle points p_1, p_2, p_3 are determined so that these points have a characteristic curvature feature as depicted in figure 3-a. Thus, p_2 is the maximum curvature point. p_1 is a zero-crossing curvature point before p_2. p_3 is a zero-crossing curvature point after p_2.

The next step regards the approximation of the two angle borders S_1, S_2. The segment S_1 is calculated following the linear least-square regression on the set of the medial axis points (ϕ) that lie between p_1 and p_2, leading to the segment equation :

$$y = \frac{Cov(x, y)}{V(x)}(x - \overline{x}) + \overline{y}$$

where $\overline{x}, \overline{y}$ are the empirical means of ϕ abscissas and ordinates respectively, $V(x)$ is the empirical variance of ϕ abscissas, $Cov(x, y)$ is the empirical covariance between ϕ abscissas and ordinates. By performing analogous computations, the second segment S_2 is computed from points that are between p_2 and p_3. Finally, the anorectal angle θ is formed by the segments S_1, S_2 and the anorectal vertex corresponds to the intersection point of these two segments.

B. Uterus-vagina

The uterovaginal angle represents the uterus inclination compared with the vagina. We have followed the same process as the one proposed for the anorectal angle approximation. Since the uterovaginal angle is generally opposite to the anorectal angle, we have selected the angle vertex to be the point which has the maximum curvature, according to the opposite direction of the curvature.

C. Bladder

Unlike the rectum and the uterus-vagina, the bladder does not have a characteristic shape. Therefore, it is difficult to define an objective criterion for the bladder neck determination. We assume that the bladder neck is the lowest point of the bladder contour. In addition, we have estimated the bladder inclination relative to the horizontal axis, this is possible thanks to the calculation of the principal axes of the shape [3]. Principal axes are deducted from the statistical moments at the second order. A moment of order p and repetition q is defined as :

$$m_{p,q} = \sum_x \sum_y (x - \bar{x})^p (y - \bar{y})^q$$

The eigenvalues related to the second order moments matrix are then computed. As a result, the inclination angle is defined as the angle between the principal axis and the horizontal axis.

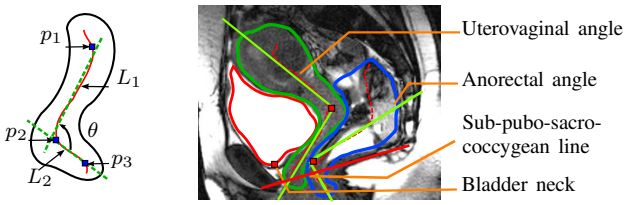

-a- -b-

Fig. 3. a- The anorectal angle definition: the computed points and segments. b- A typical result of the estimation of the anatomical references.

III. RESULTS AND DISCUSSION

We present in this section some results of the anatomical landmark approximation method we applied on the pelvic organs from a set of 30 MRI sequences. These results allow us to analyze the stability of the proposed methods, and their interest for the detection of pathologies.

A. Variablity Analysis

We have tested our methodology on sequences segmented manually by several clinicians. The variability analysis consists in the comparison of the angles and the points calculated from segmentations made by different operators departing from the same MRI sequence. This, in order to quantitatively estimate the impact of inaccuracies that may occur while segmenting the sequence, on the anatomical measurements. As indicators of the variability between two sequences, we have selected the mean distance μ between angles / points, and the standard deviation σ. Thus, for two segmentations of the same sequence S_1 and S_2 consisting of N frames, the mean is determined as follows:

$$\mu(S_1, S_2) = \frac{1}{N} \sum_{i=1}^{N} |a_1(i) - a_2(i)|$$

Where a_j is the vector of the computed angles of S_j. The standard deviation is calculated as follow:

$$\sigma(S_1, S_2) = \sqrt{\frac{1}{N} \sum_{i=1}^{N} (|a_1(i) - a_2(i)| - \mu(S_1, S_2))^2}$$

The Euclidean distance is used when dealing with the anatomical points.

Figure 4 shows for each organ the representation of the variability rates of the computed angles/points in a 2D space formed by the mean (abscissa) and the standard deviation (ordinate). All the comparisons between the available segmentations are represented. Table I recapitulates the average variability rates of all the anatomical references. Obviously, we note that the intra-operator variability is lower than the inter-operator variability. An inter-organ comparison shows that the bladder is less sensitive to the inter-operator variability than the uterus and the rectum, respectively. This is explained by the fact that the bladder is well contrasted on the MRI, while it is more difficult sometimes to delineate the contours of the uterus or the rectum. On the whole, the variability rates of the measured angles do not exceed on average 10°, reaching a maximum of 15° in some cases. The calculated points also remain stable since there is a relatively small margin (5 mm). These results allow us to consider that the impact of the segmentation variability is limited upon the anatomical measurements calculated, which validates the approach robustness.

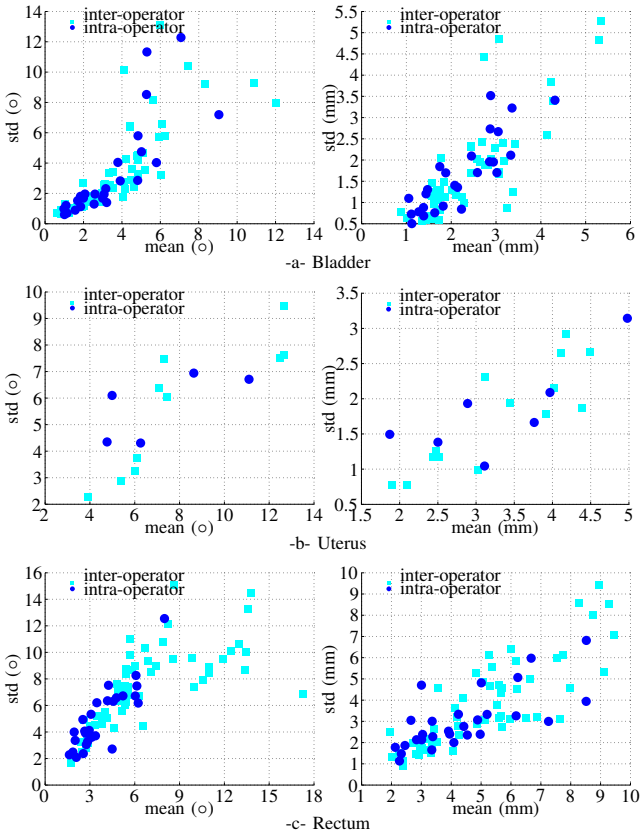

Fig. 4. Pelvic landmark approximation variability according to different segmentations

TABLE I
OVERALL VARIABILITY

	Point (mm)		*Angle (°)*	
	intra	*inter*	*intra*	*inter*
Bladder	2.20±1.65	2.40±1.78	3.37±3.33	3.88±3.63
Uterus	3.29±1.82	3.29±1.74	7.15±5.68	8.11±5.66
Rectum	4.37±3.02	5.08±3.75	6.21±5.01	11.18±7.40

B. Pathology Detection

We want to test the capabilities of the calculated anatomical references to identify pathologies related to the behaviors of the pelvic organs. To this purpose, we perform an inter-subject analysis. We have a dataset of thirty (30) MRI sequences labelled with the clinical diagnosis of each organ. We propose a compact representation of all the sequences,

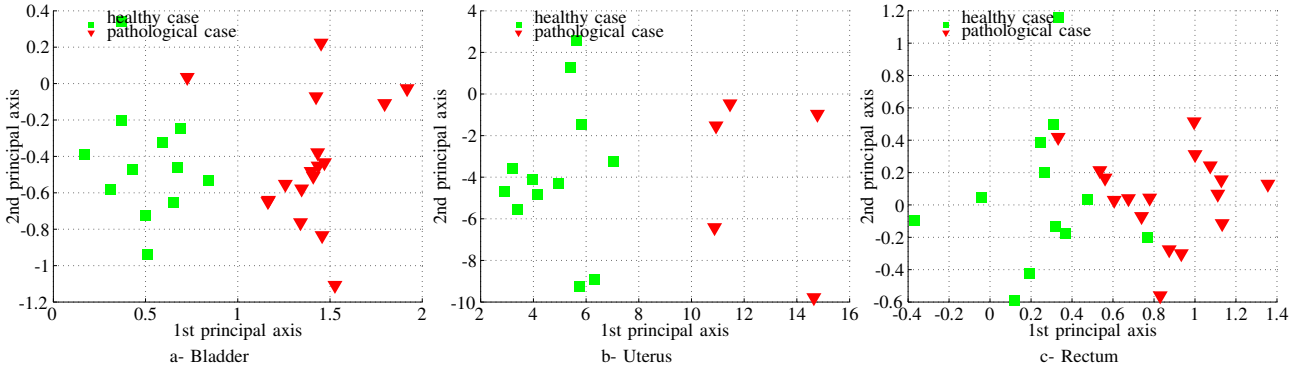

Fig. 5. Discrimination capabilities of the landmark features, by plotting the sequences according to the 1^{st} and 2^{nd} principal component.

basing ourselves on features which are extracted from the calculated references. We have noted that the variations of the anatomical angles do not charcterize a pathological organ behavior. The pelvic floor disorders are rather associated with a strong organ descent. Thus, we selected as features only the distances relative to the SPCL of the bladder neck, the uterovaginal angle vertex and the anorectal angle vertex. Those distances form the perineal descent. Each subject is then represented by a vector containing m distances between the SPCL and the points. The distances for n subjects of a given point are represented by the matrix M:

$$M = \begin{pmatrix} & & \overrightarrow{patient} & & \\ a_{1,1} & . & a_{1,2} & . & a_{1,n} \\ . & . & . & & \\ a_{i,1} & . & a_{i,j} & . & a_{i,n} \\ . & & & & \\ a_{m,1} & . & a_{m,j} & . & a_{m,n} \end{pmatrix} \downarrow time$$

Where $a_{i,j}$ is the i^{th} distance of the j^{th} patient. Figure 5 depicts the result of a representation of the perineal descent calculated on all the sequences, according to the two principal axes of inertia, computed thanks to the principal components analysis (PCA). The PCA is an exploratory data analysis method, it allows reducing data dimensions for a more compact handling. The data are projected in the space formed by the eigenvectors calculated from the covariance matrix of M. The inertia ratio is the ratio between the eigenvalue associated with the axis of inertia and the sum of all the eigenvalues, we obtained 89%, 86%, 86% for the bladder, the uterus and the rectum respectively, which is considered sufficient to validate the 2D representation. In figure 5, we can easily observe that there is a separation between the pathological cases (red triangles) and the healthy ones (green rectangles). Hence, the discrimination results, on the whole, confirm the relevance of the calculated features. Moreover, those results lead us to consider a possible diagnosis-aid tool, provided that we have a larger dataset.

IV. CONCLUSION

The determination of the anatomical landmarks and measurements are often subject to a variability, due to the limited resolution of the MRI besides subjective parameters specific to the clinician. We attempted to address this problem by providing an automatic approach to approximate these landmarks. We obtained objective elements to characterize the behavior of the pelvic organs during a strain, providing the clinicians with a measurement tool which could be automatically integrated into the radiological examination. The computed features from 30 subjects highlighted the pathological behavior of each pelvic organ, this result suggests the possibility of establishing a diagnosis-aid system, with more MRI sequences. Moreover, in order to have a fully automated process, we are working on automating the segmentation currently, using a contour tracking method. In this context, the stability analysis of the calculated landmarks showed that the segmentation variability has a limited influence on the angles and the points estimated, so we can assume that an automatic segmentation should give satisfactory results if integrated in the whole process.

V. ACKNOWLEDGMENTS

This work is supported by the French National Research Agency (ANR) under reference ANR-09-SYSC-008.

REFERENCES

[1] S. Ferrante, R. Perry, J. Schreiman, S. Cheng, and M. Frick, "The reproducibility of measuring the anorectal angle in defecography," *Diseases of the colon & rectum*, vol. 34, no. 1, pp. 51–55, 1991.

[2] J. R. Fielding, "Mr imaging of pelvic floor relaxation," *Radiologic Clinics of North America*, vol. 41, no. 4, pp. 747 – 756, 2003.

[3] R. C. Gonzalez and R. E. Woods, *Digital Image Processing*. Boston, MA, USA: Addison-Wesley Longman Publishing Co., Inc., 2001.

[4] C. Maher, K. Baessler, C. Glazener, E. Adams, and S. Hagen., "Surgical management of pelvic organ prolapse in women." *Cochrane Database of Systematic Reviews*, vol. 18, no. 4, 2004.

[5] M. Rahim, M.-E. Bellemare, N. Pirró, and R. Bulot, "A shape descriptors comparison for organs deformation characterization in mri sequences," in *International Conference on Image Processing*, 2009, pp. 1069 – 1072.

[6] E. Remy and E. Thiel, "Medial axis for chamfer distances: computing look-up tables and neighbourhoods in 2D or 3D," *Pattern Recognition Letters*, vol. 23, no. 6, pp. 649–661, 2002.

[7] R. Seynaeve, I. Billiet, P. Vossaert, P. Verleyen, and A. Steegmans, "MR imaging of the pelvic floor," *JBR-BTR*, vol. 89, no. 4, pp. 182–189, 2006.

[8] A. M. Weber and H. E. Richter, "Pelvic organ prolapse," *Obstetrics and Gynecology*, vol. 106, no. 3, pp. 615–634, 2005.